Effect of morphology and microstructure on the thermal conductivity of chalcogenide thermoelectric materials

Lian, Hong

DOI:
10.33612/diss.180380682

CHAPTER 2

Experimental Strategies

Abstract

This chapter outlines the experimental synthesis strategies and characterization techniques used in this thesis. Solid state methods were mainly used for sample preparation, and the structure and morphology of the samples were characterized using X-ray diffraction (XRD), scanning electron microscopy (SEM), and transmission electron microscopy (TEM). For each technique related to the measurement of thermoelectric properties (Seebeck coefficient, electrical conductivity, and thermal conductivity), a brief theoretical background is given.

2.1 Synthesis Methods

The materials studied in this thesis were prepared by high-temperature solid-state methods, which have the advantages of simple operation, high efficiency, and scalability to large sample sizes. Solid-state methods generally involve heating two or more substances, sometimes remaining in the solid phase and sometimes heating to the liquid phase, but allowing atoms of the reactants to diffuse and generate new materials. The raw materials used in this thesis were mostly metal or chalcogen powders, such as lead, germanium, and tellurium. Since these materials are volatile and react readily with water or oxygen in the air when heated, the raw materials in the required stoichiometric ratios were loaded in dried and/or carbon-coated quartz tubes after grinding or ball milling to mix them evenly. The tubes were then attached to a vacuum pump and sealed using a flame, as shown in Figure 2.1.

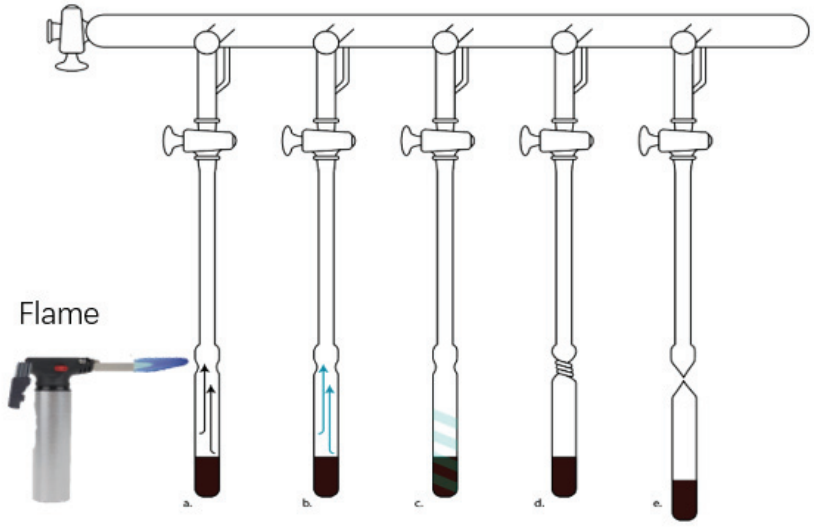

Figure 2.1 Step by step sealing of an evacuated quartz tube using a flame:
a). A vacuum is applied.
b). All residual moisture is removed by heating with a heat gun.
c). The lower end of the ampule is cooled by immersing in liquid nitrogen.
d). The neck of the ampule is softened using a hot flame and twisted shut.
e). The bottom of the ampule is pulled away from the top.
Figure by Durjan Krist.

Heating of the sealed tubes was carried out either in a tube furnace or a box furnace. In both cases, in order to obtain a uniform and crack-free sample, long-handled tongs were used to shake the quartz tube vigorously every 10 minutes during heating as shown in Figure 2.2. After cooling, following procedures that will be described for each individual sample, the obtained ingots were retrieved after breaking the ampule. The ingots were cut into pieces suitable for various measurements using a diamond wire saw.

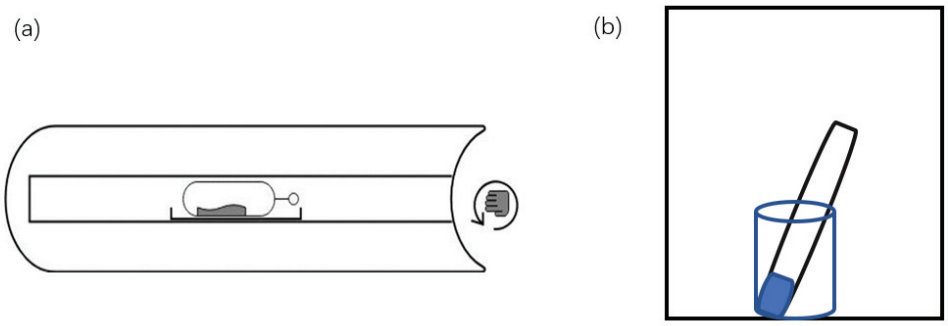

Figure 2.2 Schematic diagram of sealed quartz tube in (a) tube furnace and (b) box furnace

2.2 Structural and physical properties characterization

2.2.1 X-ray diffraction

Powder x-ray diffraction (XRD) was performed using a Bruker D8 Advance X-Ray diffractometer. A copper X-ray tube was used and measurements were performed in Bragg-Brentano geometry. The diffraction patterns obtained were fitted using the GSAS suite [65]. In some cases the ingots were ground into a fine powder for measurement, and in other cases the polished surface of the ingots was measured. All samples were handled in ambient environment at room temperature.

Single crystal XRD was performed using a Bruker D8 Venture diffractometer. Single crystals of approximate size ~200 μm were selected using an optical microscope and attached to a 0.3 mm diameter nylon loop using cryogenic oil. For low temperature measurements, the crystal was cooled to 100 K using a stream of dry nitrogen. The Bruker Apex II or Apex III software was used for data processing and initial structure solution, and the SHELX97 software was used to refine the crystal structures [66].

2.2.2 Scanning electron microscopy and energy dispersive X-ray spectroscopy

Scanning electron microscopy (SEM)[3-4] with a Everhart-Thornley secondary electron detector is a technique used to visualize the surface morphology of a sample by giving images with three-dimensional appearance. The signal used to produce images is from interactions of the electron beam with atoms at different depths within the sample. Several different types of signals can be detected: secondary electrons, reflected or back-scattered electrons, and characteristic X-rays. SEM has become an important tool for non-destructive inspection and evaluation of the surfaces of both metallic and non-metallic materials.

Secondary electrons are created due to an inelastic interaction of the electron beam with the electrons of the material. Due to the inelasticity of the interaction these electrons are of relatively low energy and hence have a short mean-free path in the material. All secondary electrons that are detected thus originate from the surface, close to the point at which the electron beam impact takes place. Therefore, it is possible to use these secondary electrons for high resolution imaging. Conversely, the backscattered electrons are created due to elastic scattering. They are of higher energy than the secondary electrons which allows a signal to be obtained from up to approximately one micron deep in the sample. The image resolution is poorer than for secondary electrons but the advantage to using backscattered electrons is that they contain information about the atoms that they interact with. Heavier atoms scatter more strongly than lighter atoms and thus provide a stronger signal at the detector. Backscattered electron images can thus provide information about the distribution of elements in the surface region of the sample, as well as the surface topography.

Characteristic X-rays are used in energy-dispersive X-ray spectroscopy (EDS). In this thesis the same equipment was used for EDS as for SEM. The incident electrons in the beam excite inner-shell electrons of atoms in the sample. The resulting holes are filled by the relaxation of electrons from higher energy levels, resulting in the emission of fluorescent X-rays which are collected by an X-ray spectrometer that measures their energy and intensity. Since the energy distribution of these X-rays reflects the electronic energy levels of specific elements, EDS spectra can be used to quantitatively determine the elemental composition of samples.

In this thesis the surfaces of the samples were polished with 500 and 800 grit sandpaper, followed by 9, 3 and 1 μm diamond suspensions. Finally, grinding with a 40 nm silica suspension was performed. In order to obtain a clear image with high contrast and resolution, many variables must be controlled including the current, voltage and spot size. The accelerating voltage must be set to an appropriate value (5-15 kV). Higher voltages will have higher resolution, resulting in most primary electrons moving deeper in the sample, the depth of which depends on the sample density and elemental composition. In this case, for most samples, the yield of secondary electrons will be lower and surface detail will be lost. On the other hand, backscattered electrons come from below the surface, so higher voltages can be used to increase the yield. Similarly, X-rays can propagate from relatively deep in the sample, hence EDS generally uses higher voltages even though the image resolution will not be as good. By selecting a smaller area and optimizing it, a good beam focus can be achieved. In this thesis, the microstructure of the samples was studied using a FEI Nova NanoSEM 650 equipped with an EDAX EDS/EBSD system using an Octane EDS detector and Hikari Plus EBSD camera. The Team v.4.5 and OIM Analysis v.8.1 software were used to perform semiquantitative EDS and electron backscatter diffraction (EBSD) data analysis, respectively.

2.2.3 Seebeck and resistivity measurements

The Seebeck coefficient and electrical conductivity were measured above room temperature using a Linseis LSR-3 setup. This machine is designed for measurements in the range 300K to 1073K under helium atomosphere, using automated data acquisition software. The temperature dependence of the Seebeck coefficient and electrical conductivity can be measured on samples of cylindrical or rectangular shape. The length of the sample should be more than 7 mm in order to successfully clamp it vertically between the upper and lower platinum electrodes. In this thesis, the as-synthesized ingots were cut into suitable rectangles using an electric diamond wire saw and then polished with 1000 mesh fine sandpaper.

A schematic picture of the measurement setup is shown in Figure 2.3:

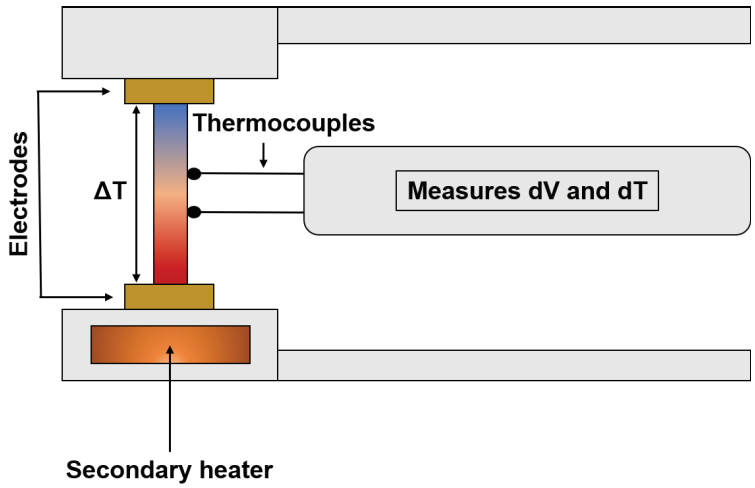

Figure 2.3 Schematic layout of Linseis LSR-3 setup. Figure by Joshua Levinsky.

There are two sources of heat in the setup. The primary furnace covers the entire measurement assembly and is used to heat the sample to a specific temperature. A secondary heater is contained in the lower electrode block and is used to generate a temperature gradient across the sample at any given measurement temperature.

The Seebeck coefficient is obtained by measuring the temperature gradient (ΔT), which is the difference between the upper and lower temperatures T1 and T2 measured by the thermocouples in mechanical contact with the sample (see Figure 2.3), and the electromotive force, dE, measured by the same wires in response to the temperature gradient. The Seebeck coefficient is then calculated as below:

$$S = \frac{\Delta V}{\Delta T} - S_{probe} \qquad (2.1)$$

The electrical resistivity is simultaneously determined using the DC 4-terminal method by applying a constant current across the sample and measuring the voltage difference between the thermocouple leads in contact with the sample, after subtracting the thermo-electromotive force between the leads. The electrical resistivity is then calculated as follows:

$$\rho = \frac{RA}{l} \qquad (2.2)$$

where A is the surface area of the sample on the side of contact and l is the distance between the probe thermocouples. In order to obtain high-quality data, before measurement it should be ensured that an appropriate temperature range is selected in order to avoid damage to the instrument in case the sample is volatile, and the surface of the sample should be smooth and fully polished.

2.2.4 Thermal diffusivity measurements

Thermal diffusivity (D_{th}) measurements were performed with the use of a Linseis XFA 600 (as shown in Figure 2.4). Thermal conductivity was calculated using the formula $\kappa = D_{th} \times \rho \times C_p$, where the density ρ was calculated from the mass and volume of the sample determined by direct measurement, and specific heat capacity (C_p) was either taken from literature reports or estimated by the Dulong-Petit approximation

$$C_p = \frac{3R}{M} \qquad (2.3)$$

where R is the universal gas constant and M is the molar mass.

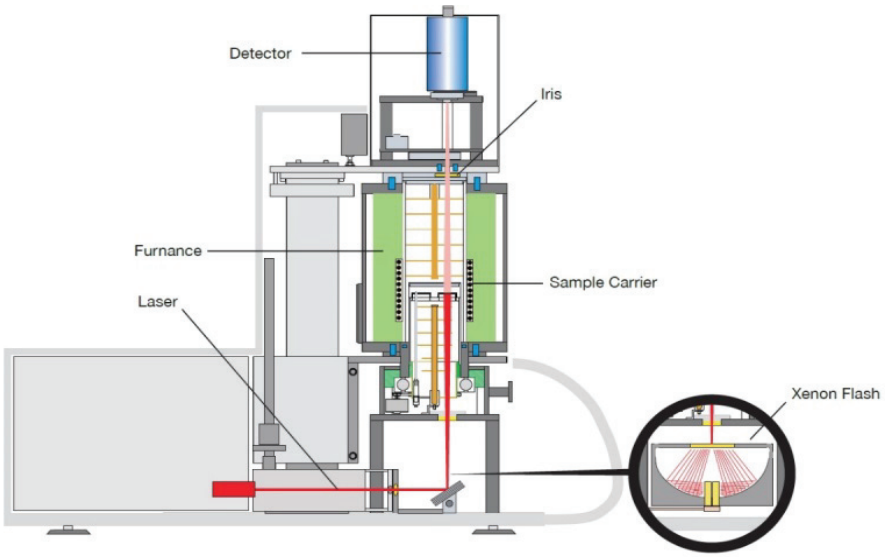

Figure 2.4 The Linseis LFA 1000 setup. Figure from the Linseis LFA 1000 manual.

This apparatus, shown in Figure 2.4, makes use of the laser flash technique where a laser pulse heats one side of a sample, and the rise in temperature as a function of time on the other side is measured with the use of a high speed IR detector. The thermal diffusivity is then calculated by using $D_{th} = 0.1388\ d^2 / t_{1/2}$, where d is the thickness of the sample and $t_{1/2}$ is the time taken to reach half of the maximum temperature. The laser flash comes from a xenon lamp and the sample is situated inside a vacuum furnace, which allows for measurements at a range of temperature. There are no special requirements for the shape and size of the polished sample to be tested, although the thickness should be less than 4 mm. Silicon carbide sample holders are available with holes of different dimensions for exposure to the laser flash. The samples should be as flat and smoothly polished as possible. The size of the sample can have a small effect on the quality and precision of the data obtained; generally, the largest possible sample should be chosen.

References

1 H. J. Goldsmid, *Introduction to Thermoelectricity*, Springer, 2010.

2 G. M. Sheldrick, *Acta Crystallogr. A*, 2008, **64**, 112.

3 M. Abd Mutalib, M. A. Rahman, M. Othman, A. F. Ismail and J. Jaafar, in *Scanning electron microscopy (SEM) and energy-dispersive X-ray (EDX) spectroscopy*, Elsevier, 2017, pp. 161-179.

4 B. J. Inkson, in *Scanning electron microscopy (SEM) and transmission electron microscopy (TEM) for materials characterization*, Elsevier, 2016, pp. 17-43.